



Contents lists available at ScienceDirect

Journal of Neuroscience Methods

journal homepage: [www.elsevier.com/locate/jneumeth](http://www.elsevier.com/locate/jneumeth)



## Characterization of trial-to-trial fluctuations in local field potentials recorded in cerebral cortex of awake behaving macaque

David L. Menzer<sup>a,\*</sup>, Hemant Bokil<sup>b</sup>, Jae Wook Ryou<sup>a</sup>, Nicholas D. Schiff<sup>a</sup>, Keith P. Purpura<sup>a</sup>, Partha P. Mitra<sup>b</sup>

<sup>a</sup> Department of Neurology and Neuroscience, Weill Medical College and Graduate School of Medical Sciences of Cornell University, 1300 York Avenue, New York, NY 10065, USA  
<sup>b</sup> Cold Spring Harbor Laboratory, 1 Bungtown Road, Cold Spring Harbor, NY 11724, USA

### ARTICLE INFO

#### Article history:

Received 27 May 2009  
Received in revised form  
11 November 2009  
Accepted 16 November 2009

#### Keywords:

Macaque  
Oculomotor  
Local field potential  
Spectral analysis  
Nonstationarity  
Trial-to-trial

### ABSTRACT

In analyzing neurophysiologic data, individual experimental trials are usually assumed to be statistically independent. However, many studies employing functional imaging and electrophysiology have shown that brain activity during behavioral tasks includes temporally correlated trial-to-trial fluctuations. This could lead to spurious results in statistical significance tests used to compare data from different interleaved behavioral conditions presented throughout an experiment. We characterize trial-to-trial fluctuations in local field potentials recorded from the frontal cortex of a macaque monkey performing an oculomotor delayed response task. Our analysis identifies slow fluctuations (<0.1 Hz) of spectral power in 22/27 recording sessions. These trial-to-trial fluctuations are non-Gaussian, and call into question the statistical utility of standard trial shuffling. We compare our results with evidence for slow fluctuations in human functional imaging studies and other electrophysiologic studies in nonhuman primates.

Published by Elsevier B.V.

## 1. Introduction

### 1.1. Trial-to-trial fluctuations in brain activity

Most of our knowledge of the relationship between brain and behavior comes from studies of the brain's physiologic or metabolic responses to various behavioral task conditions. Task-related responses have primarily been studied with functional brain imaging techniques (e.g., fMRI or PET) and electrophysiology (e.g., depth electrode recordings of field potentials or single unit activity). Because trial-to-trial variability is usually considered noise, the brain's activity is typically evaluated by averaging task responses over trials.

However, many recent studies have indicated that physiologic and metabolic brain activity is characterized by temporally correlated fluctuations that contribute to trial-to-trial variability in task-dependent responses. A study by Llinás et al. (1999) demonstrated spontaneous fluctuations in human brain activity during a rest period not involving a behavioral task, and several subsequent studies have shown task-independent, but nevertheless correlated, trial-to-trial fluctuations in signals recorded during behavioral

tasks (see below). The lack of independence of signals recorded on successive trials of an experiment could compromise the use of standard statistical methods to compare task-dependent responses on interleaved trials from different behavioral conditions. The aims of this study are to present methods for characterizing trial-to-trial fluctuations in neuronal activity recorded during a behavioral task and explain how these fluctuations could lead to violations of the assumptions of standard statistical tests used to analyze experimental data.

### 1.2. Previous studies on trial-to-trial background fluctuations

Spiking responses of cortical neurons can depend upon trial-to-trial fluctuations in neuronal activity. Recording in the visual cortex of anesthetized cats, Arieli et al. (1996) demonstrated that stimulus-evoked spiking responses of individual cortical neurons were positively correlated with stimulus-independent fluctuations of simultaneously recorded local field potential (LFP) amplitudes. Larger spiking responses were elicited by visual stimulation during intervals of high LFP amplitudes, and smaller spiking responses were observed during intervals of low LFP amplitude. This is consistent with the idea that the LFP signal is a population-level measure of neuronal activity, representing voltage fluctuations arising from synchronized synaptic activity within approximately 500  $\mu\text{m}$  of the electrode tip (Elul, 1972; Nuñez, 1995).

\* Corresponding author at: Department of Neuroscience, Brown University, Box G-LN, Sidney E. Frank Hall for Life Sciences, 185 Meeting Street, Providence, RI 02912, USA. Tel.: +1 646 670 6830; fax: +1 401 863 1074.

E-mail address: [David.Menzer@brown.edu](mailto:David.Menzer@brown.edu) (D.L. Menzer).

In the alert monkey, Hasegawa et al. (2000) showed that trial-to-trial fluctuations in the spiking activity of a subset of prefrontal cortical neurons matched trial-to-trial fluctuations in behavioral accuracy on trials from minutes earlier in a behavioral experiment. These authors also showed that trial-to-trial fluctuations in the activity of a different subset of prefrontal neurons matched fluctuations in behavioral accuracy on trials occurring minutes later in the experiment. These authors suggested that a component of the spiking activity of these prefrontal neurons may represent attention, arousal, or motivational level, rather than task-specific behavioral requirements.

Also in the alert behaving monkey, Leopold et al. (2003) showed that the gamma band (30–100 Hz) power of LFP recordings from different sites in visual cortex fluctuates coherently at low frequencies (<0.1 Hz) during both rest and task conditions. These authors suggest that low-frequency task-independent fluctuation in the power of LFP signals from brain tissue may underlie the low-frequency task-independent fluctuations in BOLD signals (Biswal et al., 1995; Fox et al., 2006a,b; Vincent et al., 2006, 2007) that occur on the same time scale, although this putative link between fluctuations in LFP power and the BOLD signal has not been proven.

### 1.3. Specific issues addressed in the present study

In this study, we examine trial-to-trial variability in LFP recordings from the frontal cortex of an alert macaque monkey performing a behavioral task. We investigate two questions regarding the trial-to-trial variability of the LFP recordings. The first question is whether the trial-to-trial variability is consistent with an underlying Gaussian stochastic process. For a stationary stochastic process, the Fourier transform at a single frequency is asymptotically Gaussian distributed (whether or not the original process is Gaussian), as long as the process does not have a very long memory. This is a result of the central limit theorem: the Fourier transform of the process is a linear sum of many random variables, and as long as correlations are sufficiently weak, the sum tends to an asymptotic Gaussian distribution. However, this does not imply that the original process is Gaussian: it may be either Gaussian or non-Gaussian. The non-Gaussianity does not manifest itself in the distribution of the complex amplitude at a single frequency (due to the central limit theorem), but in general the joint distribution of the complex amplitude at two different frequencies will show non-Gaussian behavior. Thus,  $P\{X(f_1), X(f_2)\}$  will not in general be Gaussian. If the original process is stationary, then second order correlations between two different frequencies  $f_1$  and  $f_2$  will be zero as a consequence (unless  $f_1 + f_2 = 0$ ). This does not rule out higher order correlations, as captured by the spectral power correlations we study in this paper. We reasoned that if trial-to-trial variability is consistent with a Gaussian stochastic process, then the log power estimates of the LFP separated by more than the estimation bandwidth should be uncorrelated (see section 6.6 in Percival and Walden, 1993). To evaluate this, we calculated the correlations between log power at distinct frequencies of the spectra of the LFPs recorded over the timecourse of the experiment.

The second question is whether trials in the behavioral experiment are independent for the purposes of statistical significance testing. Most statistical procedures for estimating confidence intervals assume that the LFPs from different trials of the behavioral experiment are independent. However, if the trials are truly independent, then the LFP log power estimates in a given frequency band should be uncorrelated across adjacent trials. We evaluate this second question by calculating the spectrum of trial-to-trial changes in log power in specific frequency bands. We then examine the entropy of the spectra of these trial-to-trial fluctuations in power to determine whether trial-to-trial fluctuations in a given frequency band are uncorrelated. We conclude that trial-

to-trial fluctuations in LFP log power are not consistent with an underlying Gaussian stochastic process and have substantial correlations.

## 2. Methods

### 2.1. Animal subject and surgical methods

One adult male rhesus macaque monkey (*Macaca mulatta*) was used in the study. All behavioral and electrophysiologic procedures were in compliance with the guidelines of the National Institutes of Health (NIH) and were approved by the Institutional Animal Care and Use Committee (IACUC) of the Weill Medical College of Cornell University. We prepared the animal for the experiment by behavioral training and surgical implantation of a head post adapter and a recording chamber that allowed for electrode recordings from its brain. The chamber was located at the right anterior region of the animal's skull, and was positioned to record from the right frontal eye field (FEF), located in the right arcuate sulcus.

### 2.2. Behavioral methods

We trained the animal by operant conditioning to perform an oculomotor delayed response task (Goldman-Rakic, 1987). Trials of the oculomotor delayed response task were grouped into 3 behavioral conditions (see Fig. 1). The 3 behavioral conditions were: (1) memory guided saccade (MGS) trials, (2) visually guided saccade (VGS) trials, and (3) fixation-only trials. In each of the 3 conditions, every trial began with the appearance of a central fixation point on a visual stimulus display. On ~80% of the trials (the MGS and VGS trials), the central fixation point appeared in green, and on the other ~20% of the trials, the central fixation point appeared in red (the fixation-only trials). The appearance of a green fixation point indicated to the animal that a saccade was to be made on that trial. In this case, the animal was required to maintain fixation on the fixation point for a period of 1.37 s (the baseline period of the task), before a target flashed at one location in the periphery of the visual display.

The target stimulus, a white square, subtended 2° of visual angle. The target could appear in one of eight sectors on the screen centered on the angles 0°, 45°, 90°, 135°, 180°, 225°, 270°, and 315°. The eccentricity of the target location with each sector was drawn from a uniform distribution ranging from 11° to 18° of visual angle from the central fixation point. For purposes of data analysis, we grouped locations of the target stimuli into 8 categories corresponding to its sector orientation. The target was equally likely to appear at any of these sectors.

The MGS trials constituted a randomly chosen half of the trials in which the central fixation point appeared in green (~40% of the trials, on average). In these trials, the target stimulus was flashed for 80 ms; then disappeared. Following the disappearance of the target stimulus, the animal maintained visual fixation on the central fixation spot for a variable delay period of between 1000 and 2000 ms. On ~25% of the MGS trials, the delay period lasted for 1000 ms, on ~37.5% of the MGS trials the delay period lasted for 1500 ms, and on the remaining ~37.5% of the MGS trials, the delay period lasted for 2000 ms. At the end of the variable delay period, the central fixation point extinguished, cueing the animal to make a saccade to the location in the periphery of the display where the target stimulus was flashed prior to the beginning of the delay period. If the animal made a saccade to the correct location in visual space within 800 ms, the animal was rewarded with water for a period of 300 ms.

The VGS trials constituted the other half (~40%) of the trials in which the central fixation point appeared in green. In these trials,

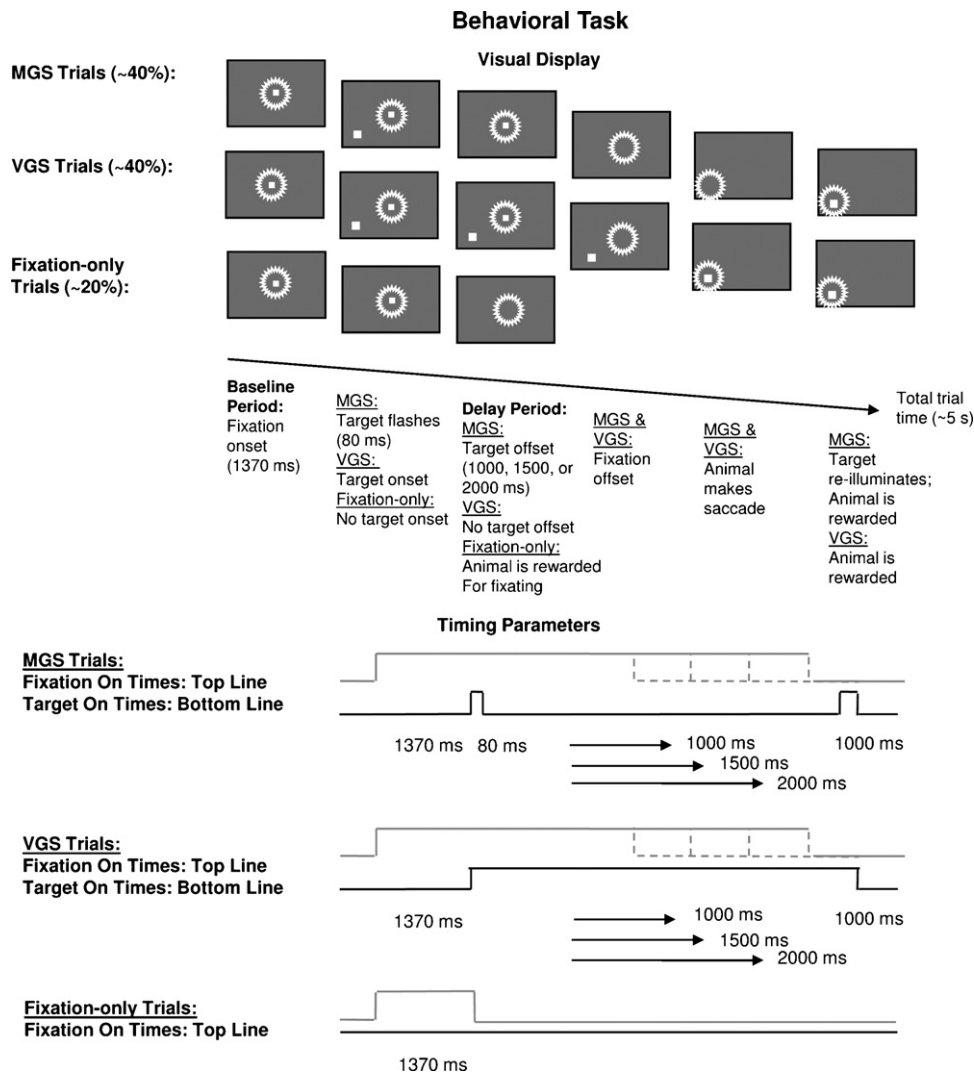


**Fig. 1.** Schematic diagram of the memory guided saccade task used in the present study.  $\odot$  symbol indicates the direction of the monkey's gaze. On the MGS and VGS trials, the fixation point was colored green. On the fixation-only trials, the fixation point was colored red.

the target stimulus was illuminated in its peripheral location but remained visible during the variable delay period. The other aspects of the trial (distribution of the delay period and reward criteria) were identical to that of the MGS trials.

In the third type of trial (fixation-only), the central fixation point appeared in red, and the animal was to maintain fixation. On these trials, the animal was rewarded for maintaining visual fixation on the central fixation spot with water for 300 ms.

We presented the trials in each of the three behavioral conditions in a randomly interleaved fashion. The animal typically completed several blocks of trials, each lasting 15 min, during an experimental session without breaks between blocks. The animal worked until fatigued or until it reached satiety. We used an infrared eye tracking system (ASL5000 IR, Applied Science Laboratories, Bedford, MA) to monitor the animal's eye position. We used TEMPO (Reflective Computing, St. Louis, MO) running on a laboratory PC to control the behavioral experiment. Visual stimuli were generated with the VSG 2/3 system (Cambridge Research Systems, Cambridge, UK) running on a separate laboratory PC and presented on a CRT (frame rate: 96 Hz; screen luminance of background gray: 78 cd/m<sup>2</sup>). Control signals for the VSG were issued by the TEMPO computer through digital i/o.

### 2.3. Neuronal recording methods

We used monopolar tungsten microelectrodes (FHC Inc., Bowdoin, ME) to record neuronal activity. The electrodes had a nominal impedance of 1.2–4 M $\Omega$  at 1 kHz. We coupled the electrodes and the electrode sheaths to single channels in an amplification system. A titanium strip anchored to one of the skull screws imbedded in the animal's head implant served as the reference ground. The electrodes were connected to a battery powered preamplifier (HS4, Tucker-Davis Technologies, Alachua, FL). The preamplifier was connected to a second amplifier (DB4, Tucker-Davis Technologies, Alachua, FL) with a fiber optic link. All channels were low-pass filtered at 7 kHz. No high pass filter was used during the experimental recordings. The gain for each channel was 8000.

The amplified voltages were sampled at 20 kHz using a data acquisition card (NIDAQ-6071E, National Instruments Corporation, Austin, TX) and streamed to disk using LabVIEW (National Instruments Corporation, Austin, TX) running under Windows 2000 (Microsoft Corporation, Redmond, WA). The data-streaming machine recorded the neuronal activity, outputs from the eye tracker and visual stimulation system, and timing signals and other behavioral flags produced by TEMPO.

#### 2.4. Confirmation of recording locations

We estimated the cortical sites of the microelectrode recordings using a 3D computer model derived from coregistered MRI and CT scans. The results of this anatomical analysis showed that the tip of the recording electrode was located in the periaruate cortex on 10/27 recording sessions and in the anterior cingulate cortex on 17/27 recording sessions. Because the results of the analyses presented in this paper were indistinguishable when the data were separated by recording location, we present the data from all 27 recording sessions together.

#### 2.5. Data conditioning and artifact removal

We performed all aspects of conditioning data for analysis and analysis of the electrophysiologic and behavioral data in MATLAB. We employed an algorithm described by Hudson (2006) to detect movement-related artifacts in the LFP data. We removed trials with movement-related artifacts from the analysis.

We used only the data from rewarded MGS and VGS trials. We did not analyze the data from the fixation-only trials, as the fixation-only trials were included as catch trials to ensure that the animal attended to the task at all times. We also dropped from the analysis trials during which the animal failed to execute the correct eye movement within the allotted time.

#### 2.6. Data analysis

The overall goal of the analysis methods developed here is to characterize trial-to-trial fluctuations in local field potentials recorded during the baseline and delay periods of each trial of the oculomotor delayed response task. We studied correlations between fluctuations in power at different frequencies, as well as temporal variations of power in a given frequency band.

Spectral analysis was applied to the LFPs to provide a quantification of the dominant frequencies of extracellular voltage fluctuations produced during the memory guided saccade task. All spectral quantities were computed with the Chronux toolbox for MATLAB (available at <http://www.chronux.org>).

#### 2.7. Application of multitaper spectral analysis to LFP data

We downsampled the recorded voltages to a sampling rate of 1 kHz. This provided a temporal resolution of 1 ms. For purposes of analysis, we took 1000 ms of LFP recorded during the first 1000 ms of each trial as the baseline period LFP. We took the first 1000 ms of LFP after the first onset of the target stimulus as the delay period LFP. In order to isolate trial-to-trial fluctuations around the average LFP response, we computed a residual LFP voltage time series  $X_{resid(n)}(t)$  for the baseline and delay periods of each trial. We computed this residual LFP separately for the LFPs from each target location in order to control for any directionally dependent visual responses to the cue. We performed this computation by taking the average of the raw voltage across trials and subtracting the average from each observation in  $X(t)$ , in the following manner:

$$X_{resid(n)}(t) = X_{(n)}(t) - \langle X(t) \rangle_N \quad (1)$$

for  $X^{\text{base}}$  and  $X^{\text{delay}}$  for each trial  $n$ , where  $\langle X^{\text{base}}(t) \rangle_N$  denotes an average across all trials  $n = 1, 2, 3, \dots, N$  for the baseline period and  $\langle X^{\text{delay}}(t) \rangle_N$  represents the average for the delay period. An example dataset showing the raw LFP  $X(t)$  averaged over MGS trials is shown in Fig. 2. The outer ring of the plot shows LFPs averaged over trials during which the target appeared in each of the 8 different target sectors in the visual display. The middle plot shows the raw LFP averaged over all target sectors.

We used non-parametric multitaper spectral estimation (Thompson, 1982; Percival & Walden, 1993) to explore the data for temporally correlated trial-to-trial fluctuations in the residual LFP signals  $X_{resid}(t)$ . We carried out our analyses separately for the LFPs recorded during the baseline and delay periods of the behavioral task.

In the multitaper method, estimation of the spectrum relies upon the multiplication of each trial of the time series data by  $K$  different orthogonal data tapers. The modulus squared of the FFT of the product of a time series and a taper is referred to as an eigenspectrum, and is denoted  $\hat{S}_k^{(mt)}(\cdot)$ . The  $K$  eigenspectra are averaged together to create a multitaper spectral estimate, which contains less variance than any single eigenspectrum because the tapers are orthogonal. The  $K$  eigenspectra can then be considered as  $K$  approximately independent estimates of the spectrum.

The tapers are formed by calculation of discrete prolate spheroidal sequences, or Slepian sequences. The Slepian sequences with parameters  $N$  and  $W$  are sequences of length  $N$  that have their energy maximally concentrated in the frequency interval  $[-W, W]$ . When Slepian sequences are used as data tapers, increases in the bandwidth  $[-W, W]$  allow for inclusion of more tapers in the spectral estimate, which leads to decreases in the frequency resolution of the spectra and increases in the bias of the spectral estimates. The half-bandwidth used in multitaper spectral estimation,  $W$ , is usually chosen by examining estimates on the same dataset using different values for  $W$ . The aim of this procedure is to choose a value for  $W$  that reduces the bias or spectral leakage within the spectrum without overly distorting the spectrum due to estimation bias.

The time-bandwidth product,  $NW$ , was chosen to be 3. The window size,  $N$ , was chosen to be 1000 ms. Thus the bandwidth of the spectral estimates was  $\pm 3$  Hz, and the value for  $\Delta t$  was .001. The number of tapers used in the multitaper method,  $K$ , is determined by the rule:  $2NW - 1$  (Thompson, 1982; Mitra and Pesaran, 1999). Thus, we used  $K = 5$  dpss tapers in the present study.

The direct multitaper spectrum estimator is given by:

$$\hat{S}_k^{(mt)}(f) = \Delta t \left| \sum_{t=1}^N h_{t,k} X_t e^{-i2\pi f t \Delta t} \right|^2 \quad (2)$$

for

$$\hat{S}^{(mt)}(f) = \frac{1}{K} \sum_{k=0}^{K-1} \hat{S}_k^{(mt)}(f) \quad (3)$$

where  $\{h_{t,k}\}$  is the data taper used when computing the  $k$ th direct spectral estimate,  $\hat{S}_k^{(mt)}(\cdot)$ .

We computed the multitaper residual LFP spectra for the baseline and delay periods for each trial. The Fourier transforms used to compute the direct spectral estimators were calculated using a padded FFT. We converted the LFP spectra to decibels (dB),  $10 \times \log_{10}(S)$  for plotting and statistical analysis. We used the log of the spectrum because taking the log equalizes estimation variance across frequencies in the spectrum (Percival and Walden, 1993).

#### 2.8. Examining trial-to-trial fluctuations by studying correlations between different frequencies

We first investigated whether the trial-to-trial variability in residual LFP log power is consistent with an underlying Gaussian stochastic process. If so, then the residual LFP log power estimates for frequencies separated by more than the bandwidth  $[-W, W]$  should be uncorrelated. To examine the data for the presence of correlations between log power estimates at different frequencies over the course of successive trials of the experiment, we calculated a correlation matrix of residual LFP log power at different frequen-

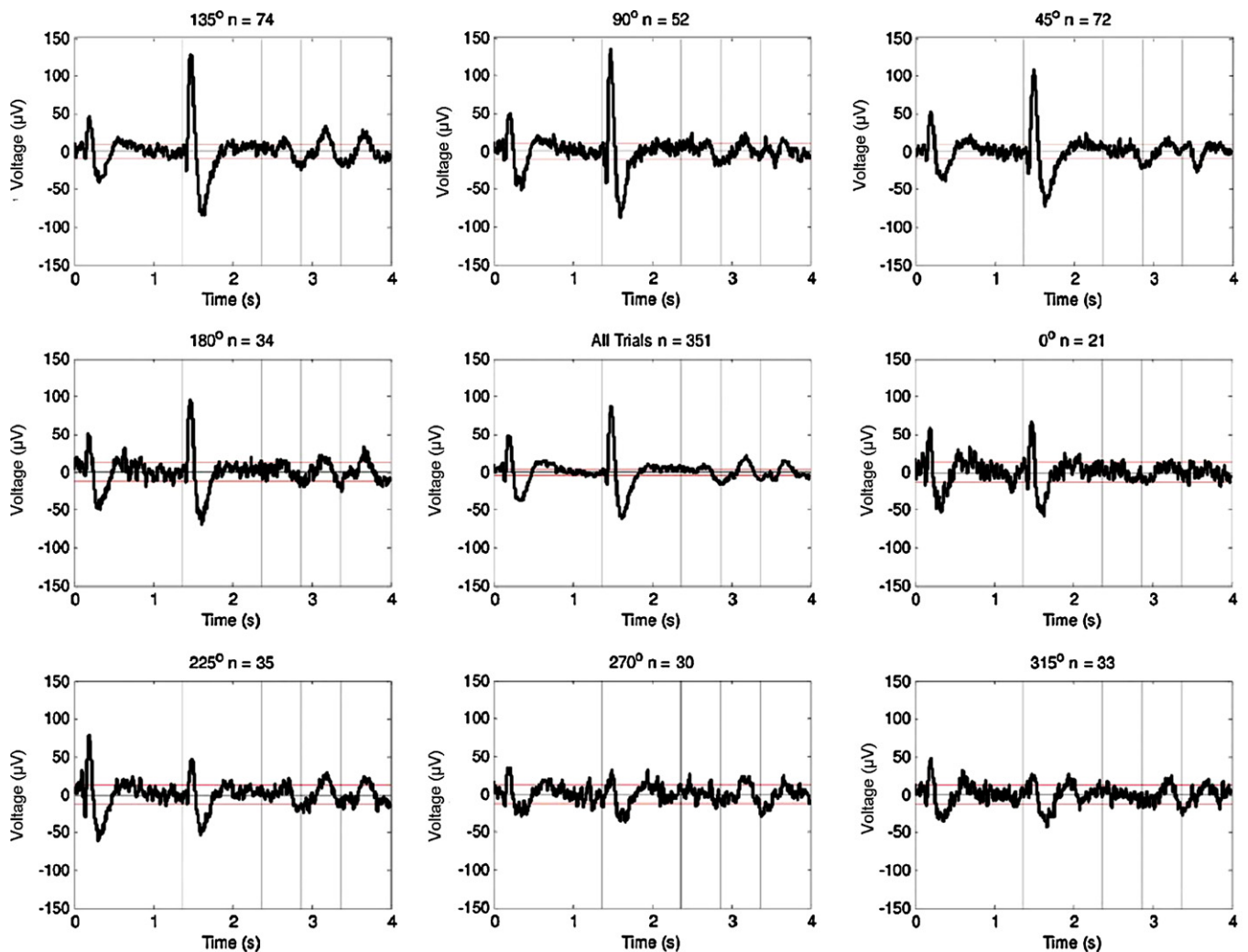


**Fig. 2.** Raw LFP voltages averaged over trials at each of 8 different target locations (outer ring of plot), and all trials (middle plot) for MGS trials during one experimental session. Time 0 indicates the start of each trial. For each plot, the vertical line at 1.37 s indicates the start of the delay period. The vertical lines at 2.37 s, 2.87 s, and 3.37 s indicate the end of the delay period for trials with 1 s, 1.5 s, and 2 s delay periods, respectively. The horizontal lines show that standard deviation of the LFP series over trials. Trial numbers are indicated by *n*.

cies for the residual LFPs. We calculated one correlation matrix for the baseline period and one correlation matrix for the delay period for each of the 27 recording sessions.

As described in Section 2.7, we calculated the residual LFP by subtracting the mean of the LFP voltages across trials from the LFP voltages recorded on each trial of the experiment. This allowed us to analyze trial-to-trial variability in the LFPs. We then calculated the log power spectrum for each trial's residual LFP using the multitaper method. Next, we calculated the mean of the log power estimates at each frequency across trials. We then subtracted the mean of the log power estimates across trials from the power spectral estimate from each trial. This step allowed us to examine fluctuations in residual LFP log power on a trial-to-trial basis over the timecourse of each experimental session. The correlation between log power at two frequencies is represented by the following equation:

$$\rho_{f,f'} = \frac{E((\log S(f) - \mu_{\log S(f)})(\log S(f') - \mu_{\log S(f')}))}{\sigma_{\log S(f)} \sigma_{\log S(f')}} \quad (4)$$

The results showed significant correlations in log power between different frequencies of the spectra of the residual LFPs for both the baseline and delay periods. The majority (22/27) of the recordings showed significant correlations in log power throughout

the high frequency range (>30 Hz) of the baseline period. Similarly, a majority (20/27) of the recordings showed significant correlations in high frequency power of the delay period. An example of the typical result for the correlation matrix of residual LFP log power for one recording's baseline and delay period activity is shown in Fig. 3. The results show significant correlations between fluctuations in residual log power in the 14–30 Hz (beta), 30–60 Hz (low gamma), and 60–200 Hz (mid gamma to high frequency) ranges of the LFP spectra. This pattern emerges for both the baseline and delay period residual LFPs, although the result for the baseline period residual LFP is noticeably more robust, as was seen in many of the recording sessions.

Additionally, in 15/27 of the baseline period and 14/27 of the delay period recordings, discrete correlations were found between harmonically related frequencies, with the fundamental frequency ranging from 20 to 40 Hz, indicating non-sinusoidal waveforms in the residual LFP. An example of this less common result is shown in Fig. 4. In this example, the correlation matrix for the baseline period shows discrete correlations between frequencies in the 30–60 Hz (low gamma) and 90–200 Hz (high gamma and high frequency) bands. The correlation matrix for the delay period residual LFP shows a similar pattern, however the result is again less robust.

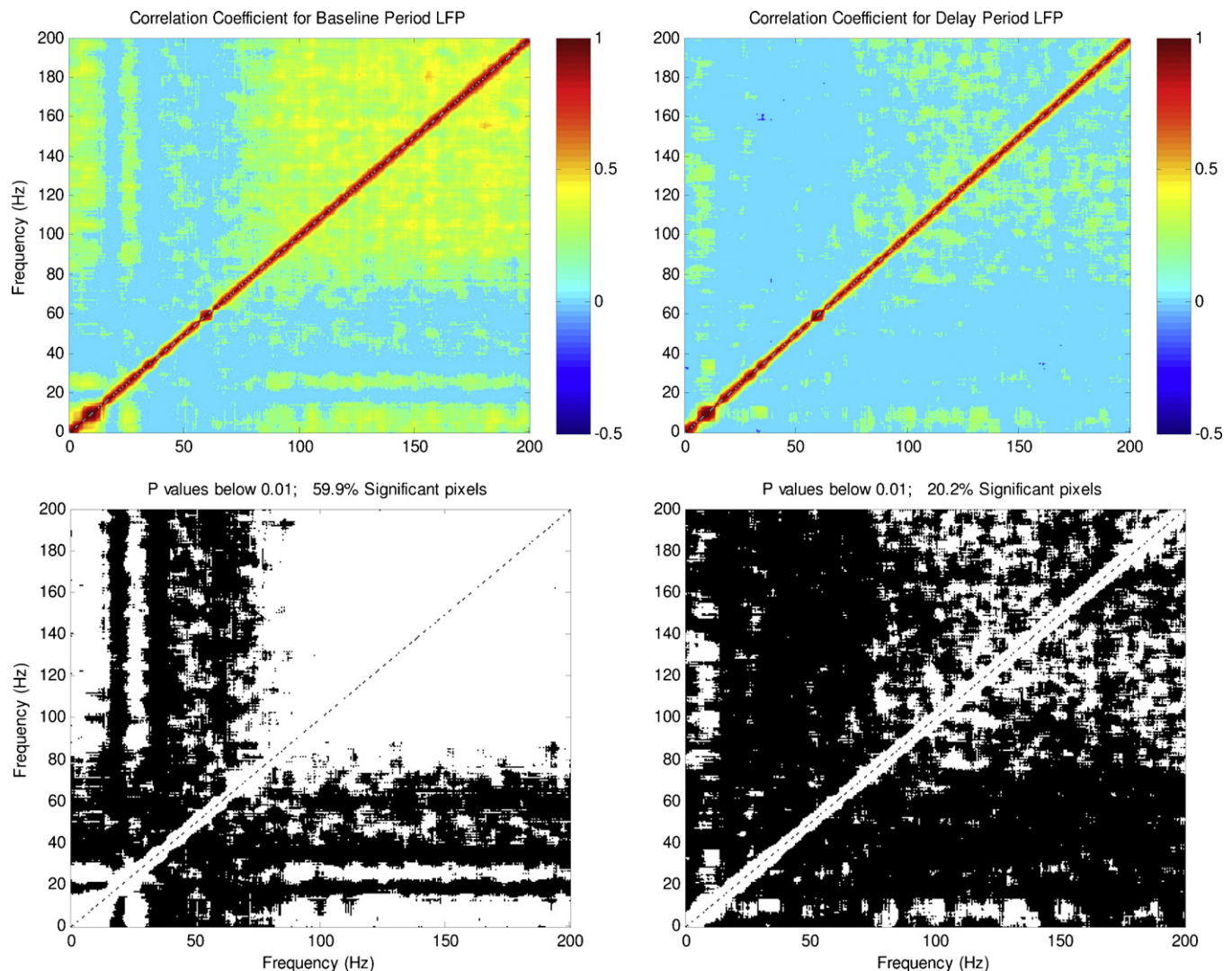


**Fig. 3.** Correlations between log power fluctuations at different frequencies in the 1–200 Hz range in the residual LFP spectra. This plot shows the typical results of our analysis, observed on 22/27 baseline period and 20/27 delay period recordings. Top left panel shows the correlation matrix for the baseline period residual LFP (1–1000 ms of each trial). Significant correlations appear in the 14–30 Hz, 30–60 Hz, and 60–200 Hz ranges of the spectrum. Top right panel shows the correlation matrix for the delay period residual LFP (1370–2370 ms of each trial). The same pattern of results emerges for the delay period data, although results are less robust. Bottom left and bottom right panels show the pixels in the top panels that are significant at alpha level 0.01.

Finally, in a minority (5/27) of the recordings from the baseline period and a minority (7/27) of the recordings from the delay period, there was no evidence of correlations of spectral estimates across frequencies. An example of this minimal effect is shown in Fig. 5. Although some nonzero correlations appear sparsely between frequencies in the 130–200 Hz range, the pixels in the correlation matrix in this example are not significant at rates exceeding the ~5% expected by chance.

A summary of the results of this analysis for the LFPs from the baseline and delay periods of each of the 27 different recording sessions is shown in Fig. 6. These results suggest that trial-to-trial variability in fluctuations of LFP power during both the baseline and delay periods is not consistent with a Gaussian stochastic process, because residual LFP power estimates for frequencies separated by more than the smoothing bandwidth generally were correlated.

### 2.9. Correlated power variations from-trial-to-trial

We next examined whether the residual LFP log power fluctuations in specific frequency bands are correlated across trials. This question is important because most statistical procedures

employed to estimate confidence intervals assume that the LFPs from different trials are independent. These statistical procedures include trial shuffling, bootstrapping, and permutation tests. If LFPs from different trials of an experiment are truly independent, then the log power estimate in a given frequency band should show uncorrelated fluctuations across trials. In a recording in which fluctuations in power are uncorrelated over time, the log power estimate in a given frequency band for one behavioral epoch of each trial (e.g., baseline or delay), plotted against trial number, should be a white noise process with a flat power spectrum.

For each of the 27 recording sessions, we examined whether trial-to-trial fluctuations in log power are uncorrelated by plotting the log power in each of 8 different frequency bands as a function of trial number in the behavioral experiment. The LFPs recorded during the baseline and delay periods of the behavioral task were analyzed separately. We separated the power of the residual LFP from the baseline and delay periods into the following 8 different frequency bands: 1–3.5 Hz (delta band), 3.5–8 Hz (theta band), 8–14 Hz (alpha band), 14–30 Hz (beta band), 30–60 Hz (low gamma band), 60–90 Hz (mid gamma band), 90–130 Hz (high gamma band), and 130–200 Hz (high frequency band). These fre-

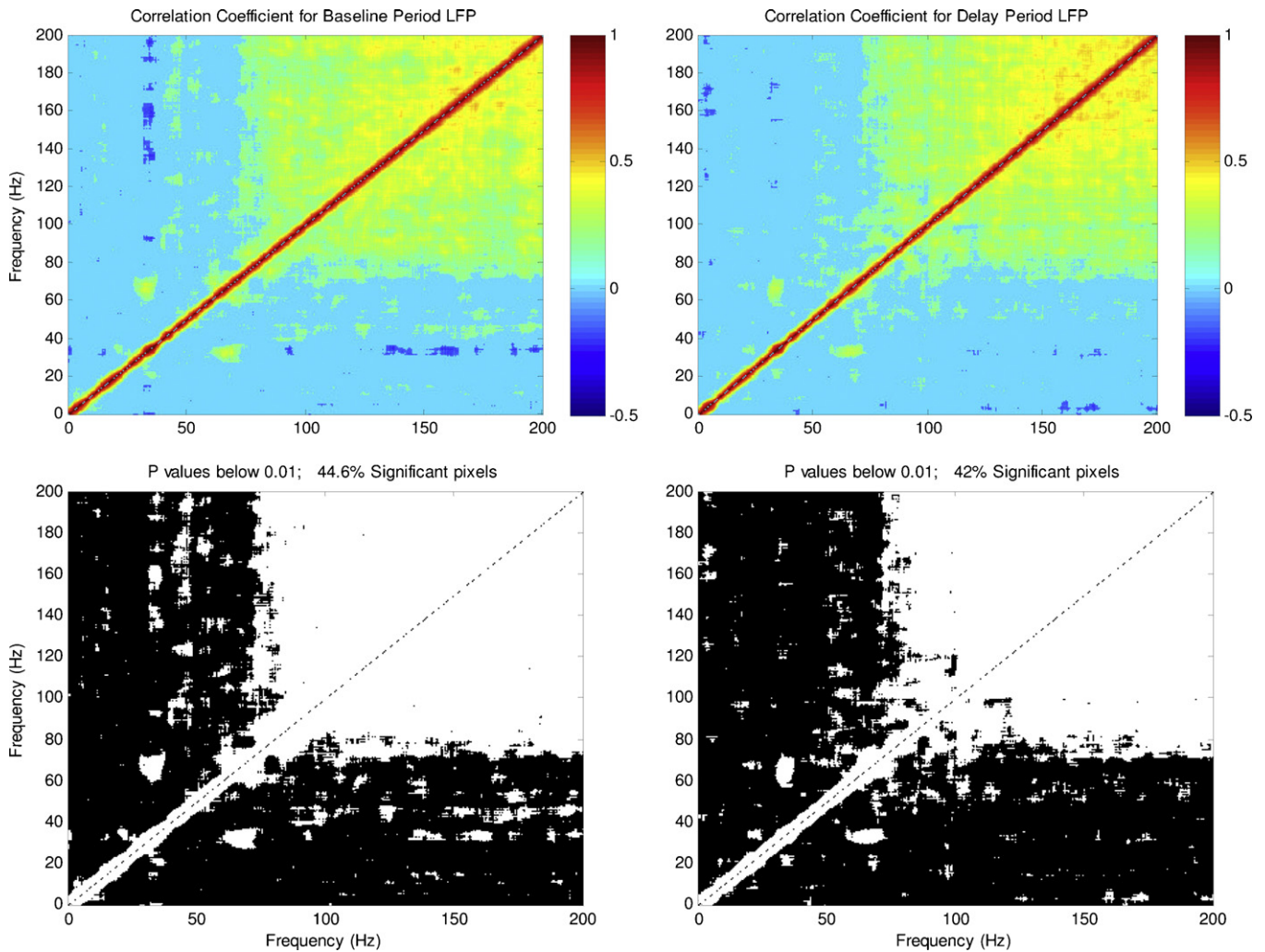


**Fig. 4.** Correlations between log power fluctuations at different frequencies in the 1–200 Hz range in the residual LFP spectra. This figure shows a less common result of our analysis, observed on 15/27 baseline period recordings and 14/27 delay period recordings. Top left panel shows an example of the correlation matrix for baseline period residual LFP spectra in which discrete correlations appear between frequencies in the 30–60 Hz and 90–200 Hz ranges. Top right panel shows a similar pattern of results for the residual LFPs recorded during the delay period of the task, although the results are less robust. Bottom left and right panels show the pixels in the top panels that are statistically significant at alpha level 0.01.

quency bands were chosen because they correspond to the bands typically used to analyze EEG recordings in humans. We separated the residual LFP log power spectra into the 8 different frequency bands after calculating the multitaper power spectrum of the residual LFP for all frequencies up to the Nyquist limit, then averaging over the log power estimates for each frequency contained in each of the 8 frequency bands separately. This yielded one number representing log power in each of 8 different frequency bands for the baseline and delay period LFPs from each trial of the experiment.

We plotted a time series of average log power estimates from the baseline and delay periods of each trial for each of the 27 different recording sessions. An example of the typical results in the 60–90 Hz frequency band on one day of recording is shown in Fig. 7. The top left panel of Fig. 7 shows the average log power in the 60–90 Hz range of the residual LFP from the baseline period of each trial. The middle left panel of Fig. 7 shows the average log power in the 60–90 Hz range of the residual LFP from the delay period of each trial. The bottom left panel of Fig. 7 shows the difference between these two time series. In the left column of Fig. 7, the trial-to-trial fluctuations in residual LFP power in the 60–90 Hz range show clear evidence of gradual changes over time. However, the difference between the log power observed during the delay vs.

baseline periods of each trial shows no evidence of gradual changes over time.

The correlated log power variations from trial-to-trial are quantified in the right column of Fig. 7. The top right panel shows the power spectrum of the time series of baseline period trial-to-trial fluctuations in average log power. This spectrum of a spectrum shows a clear peak in the low-frequency range, indicating reliable low-frequency (<0.1 Hz) fluctuations log power of the residual LFP occurring over the timecourse of the experimental session. To assess whether or not the trial-to-trial variability is consistent with a white noise process, we calculated the Wiener entropy of the spectrum of trial-to-trial power fluctuations. The equation used to calculate the log Wiener entropy is:

$$\log W = \frac{1}{N} \sum_f \log S(f) - \log \left( \frac{1}{N} \sum_f S(f) \right) \quad (5)$$

where  $f$  is the frequency in the spectrum of the spectrum of trial-to-trial fluctuations.

Values for log Wiener entropy near zero indicate a white noise process, and values for log Wiener entropy that deviate from zero

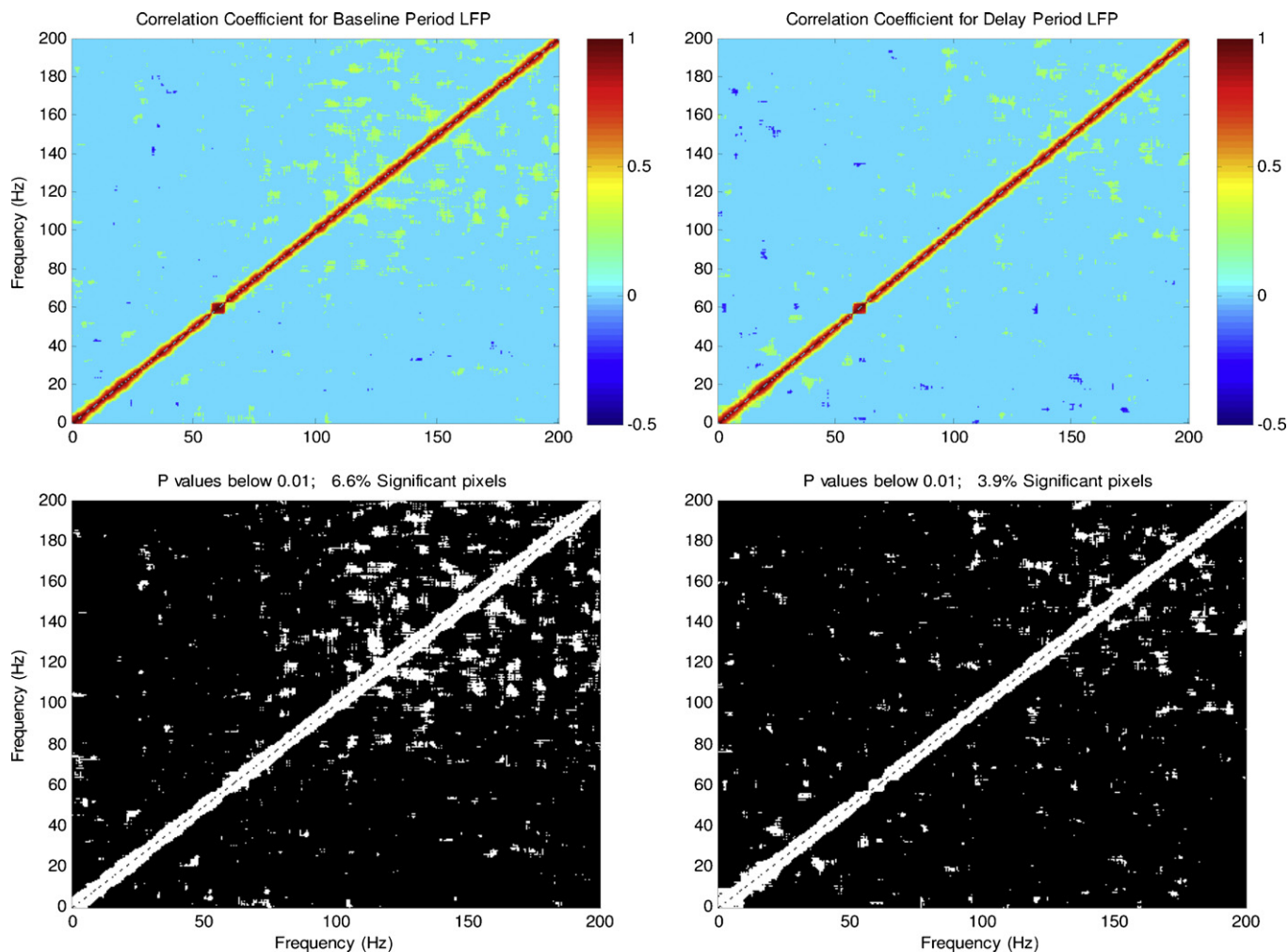


**Fig. 5.** Correlations between log power fluctuations at different frequencies in the 1–200 Hz range in the residual LFP spectra. This plot represents an absence of the typical result of this analysis. An absence of the typical results was seen on 5/27 baseline and 7/27 delay period recordings. The top panels show sparse correlations in the 130–200 Hz range. The bottom panels indicate the pixels in the top panels that are statistically significant at alpha level 0.01. Note that pixels in the correlation matrices are not significant at levels exceeding ~5%.

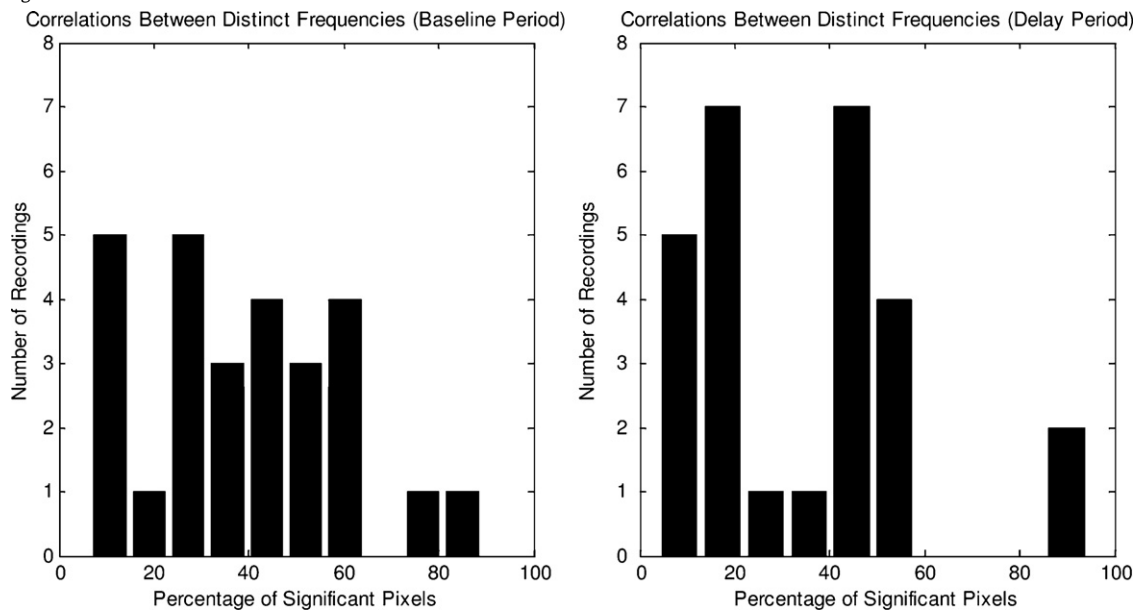


**Fig. 6.** Summary of correlations between log power fluctuations at different frequencies in the residual LFP spectra. This figure shows a summary of results across entire dataset of 27 recordings. Trial-to-trial variability in fluctuations of residual LFP log power during baseline and delay periods is not consistent with a Gaussian stochastic process, because power estimates for frequencies separated by more than the smoothing bandwidth are usually correlated. Correlations between frequencies during the delay period are usually less common, possibly due to an overall reduction in delay vs. baseline period LFP power in most recording sessions.

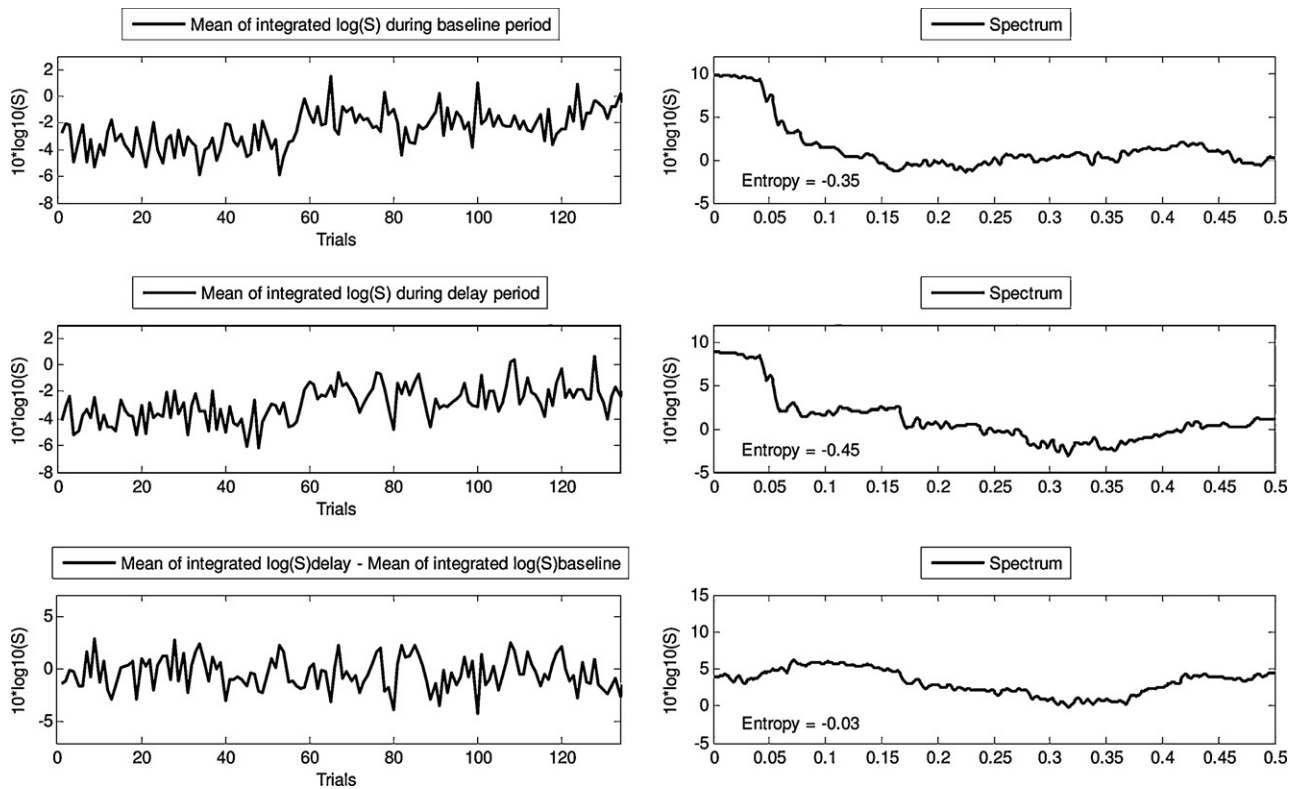


**Fig. 7.** Correlated power variations from trial-to-trial at high frequencies. This figure represents the typical result of our analysis for the 60–90 Hz band, observed on 22/27 recording sessions. Left column shows the average log power during baseline (top) and delay (middle) periods of 140 trials during 1 run of the experiment. For example, for trial 50 in the top left panel, the average power from 1 trial in the band 60–90 Hz from 1 s of baseline is plotted as a single number. The difference between average log power on each trial's delay vs. baseline period is shown in the bottom left panel. There is evidence for long-term trends in power during baseline and delay, but not in the series of delay minus baseline period log power. Right column shows the spectrum of trial-to-trial fluctuations in log power during baseline (top) and delay (middle) periods. The bottom right panel shows the spectrum of trial-to-trial series of delay vs. baseline period log power. Note the low-frequency peak in the spectra of baseline and delay period trial-to-trial fluctuations in log power.

indicate fluctuations that are correlated over time. The theoretical significance of the Wiener entropy is that it is the ratio of the residual variance of one-step linear prediction for the process, divided by the process variance. A white noise process is linearly unpredictable and therefore has Wiener entropy equal to one, because the residual variance equals the process variance. For a linearly predictable process, the residual variance after linear prediction (and therefore the Wiener entropy) is zero. The more linearly predictable the process, the more negative is the log Wiener entropy.

The Wiener entropy for the power spectrum of baseline period trial-to-trial fluctuations in the example dataset is shown in the top right panel of Fig. 7. The deviation of this entropy from zero indicates that trial-to-trial variability in baseline period log power in the 60–90 Hz range is correlated. The spectrum of trial-to-trial fluctuations in log power from the delay period of the task and its entropy are shown in the right middle panel of Fig. 7. This result shows that trial-to-trial variability in log power from the delay period in the 60–90 Hz range is also correlated. Similar to the spectrum of trial-to-trial fluctuations in baseline period log power, the peak in the low-frequency range of the spectrum indicates the presence of low-frequency fluctuations (<0.1 Hz) in log power of the LFP.

The spectrum of trial-to-trial fluctuations of the difference between delay and baseline period log power is noticeably flatter than the spectra of either the baseline or delay period fluctuations. This difference spectrum and its entropy are shown in the bottom right panel of Fig. 7. The entropy of the spectrum in the bottom right panel shows a small deviation from zero, indicating that the difference between trial-to-trial fluctuations during the delay vs. baseline periods is roughly uncorrelated over time. The fact that the

difference between delay and baseline fluctuations in the 60–90 Hz band is roughly uncorrelated indicates that the correlated fluctuations in LFP log power observed in the 60–90 Hz range during the baseline and delay periods occur comparably during both periods of the task.

Fig. 8 shows the trial-to-trial fluctuations of residual LFP power in the 3.5–8 Hz band in the same dataset used for Fig. 7. The data in Fig. 8 show no evidence of correlated trial-to-trial fluctuations in LFP power in the 3.5–8 Hz range of this example dataset. This result is typical of our recordings, demonstrating that correlated trial-to-trial fluctuations in baseline and delay period LFP power tend to occur at high frequencies in the gamma and high frequency bands, and are absent at lower frequencies.

Fig. 9 shows the results obtained on a different day of recording, in which trial-to-trial fluctuations in residual LFP power are uncorrelated in the 60–90 Hz (mid gamma) band. This figure represents an atypical result, obtained on 5/27 recording sessions. In these atypical recording session results, trial-to-trial fluctuations in residual LFP power were generally uncorrelated in each of the 8 different frequency bands.

A summary of the results of this analysis for each of the 27 different recording sessions is shown in Fig. 10. Two results are of note. First, correlated trial-to-trial variability in residual LFP power is noticeably more common at frequencies above 30 Hz than at frequencies below 30 Hz. This result is consistent with the demonstration in Section 2.8 that trial-to-trial fluctuations in LFP power are especially strong at frequencies above 30 Hz. Second, the distribution of Wiener entropies for the difference between trial-to-trial fluctuations in delay vs. baseline log power is tightly clustered around zero, indicating that the correlated trial-to-trial fluctuations

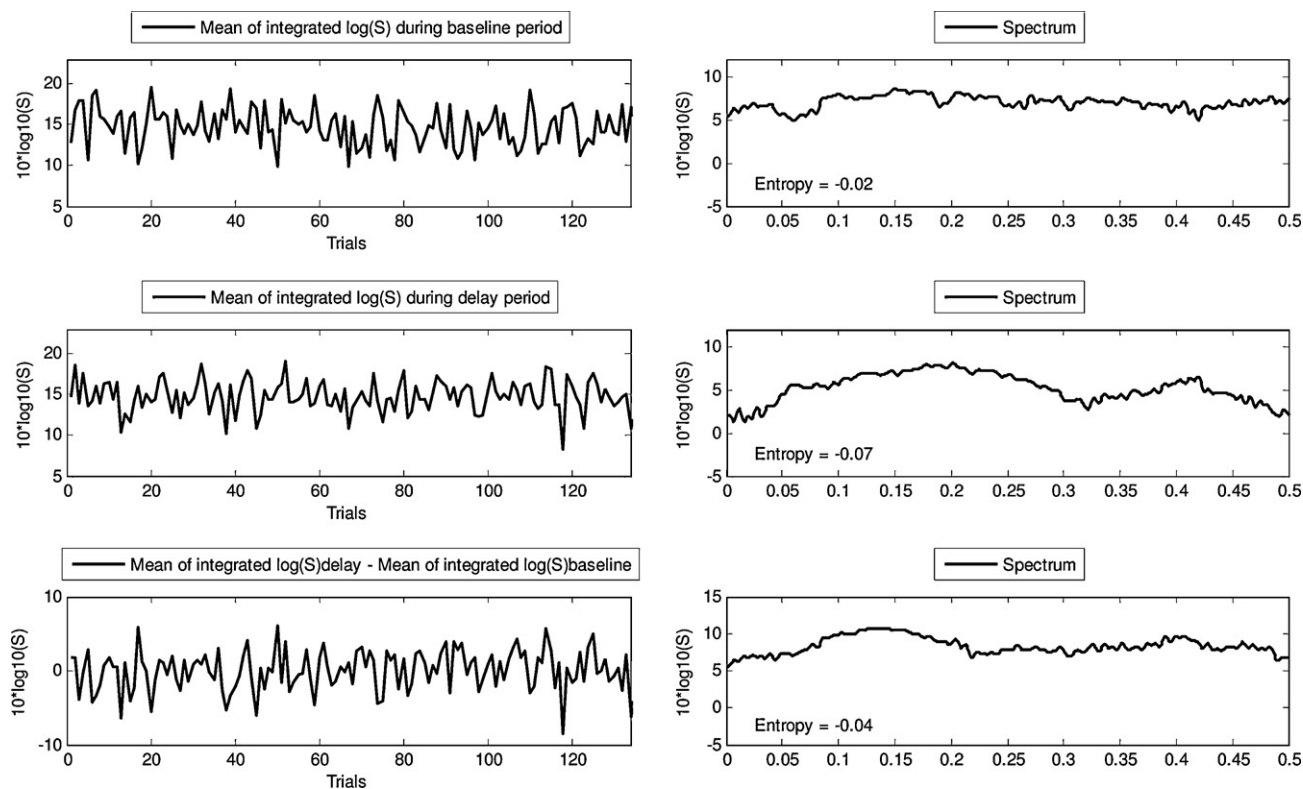


**Fig. 8.** Absence of correlated power variations from trial-to-trial at lower frequencies. This figure represents the typical result of our analysis for the 3.5–8 Hz frequency band, observed on 20/27 recordings. Figure shows power variations in the 3.5–8 Hz band from the same dataset used in Fig. 7. Left column shows trial-to-trial fluctuations in baseline (top) and delay (middle) periods. Bottom left panel shows trial-to-trial fluctuations in the difference between delay vs. baseline log power. Right column shows the spectrum of trial-to-trial fluctuations in log power observed during the baseline (top) and delay (middle) periods of the task. Bottom right panel shows the spectrum of the trial-to-trial series of the difference between delay vs. baseline period log power. Note the absence evidence for long-term trends in log power over the course of the experiment.

in LFP power occur roughly equally during the baseline and delay periods of the behavioral task.

In sum, these results indicate that the trial-to-trial fluctuations of LFP power at high frequencies during the baseline and delay periods are correlated across trials in the majority of recording sessions and call into question statistical procedures that assume that trial-to-trial variability is uncorrelated across the timecourse of an experimental session. The consequences of these findings for the use of statistical procedures that assume independence of trials will be discussed further in Section 3.3.

### 3. Discussion

#### 3.1. Main findings of the present study

There are two main findings of this study. The first finding is that trial-to-trial variability of LFPs recorded from the cortex of an alert behaving rhesus monkey is not consistent with a Gaussian stochastic process, because log power at distinct frequencies of the spectra of the LFPs recorded over the timecourse of an experiment are significantly correlated. The second finding is that trials of the behavioral experiment are not independent for the purposes of statistical significance testing, because the LFP log power estimate in a given frequency band typically shows correlated trial-to-trial fluctuations. Such correlated fluctuations are more common at frequencies above 30 Hz.

#### 3.2. Relation to previous studies of task-independent fluctuations

The results of the present study demonstrate task-independent fluctuations in LFP power, a measure of brain activity that specifi-

cally reflects neuronal activity. The present findings are consistent with those of Leopold et al. (2003), who showed low-frequency (<0.1 Hz) task-independent fluctuations in the power of LFPs recorded in the visual cortex of alert rhesus monkeys.

#### 3.3. Implications for statistical significance testing

Most of the common methods for estimating confidence intervals, including trial shuffling, bootstrap, and permutation tests assume that different trials from a behavioral experiment are independent. This is because trial-to-trial variability is usually assumed to be a Gaussian stochastic process. ANOVA, a common method of comparing signals from different interleaved behavioral conditions in an experiment, also assumes that trial-to-trial variability is consistent with a Gaussian stochastic process (Eisenhart, 1947). Our study demonstrates that these assumptions are not met in a dataset of LFP recordings in the alert behaving macaque. Thus, non-Gaussian fluctuations in local field potentials could compromise the use of standard statistical techniques for computing confidence intervals or comparing data from different experimental conditions. Recent advancements such as the Local Block Bootstrap (Papadimitis and Politis, 2002) may be preferable for estimating confidence intervals when substantial trial-to-trial variability is present.

#### 3.4. Importance of non-Gaussianity as a property of physiologic data

The importance of non-Gaussian behavior in studying physiologic signals is that such non-Gaussianity may result from physiologically important processes, such as switching between

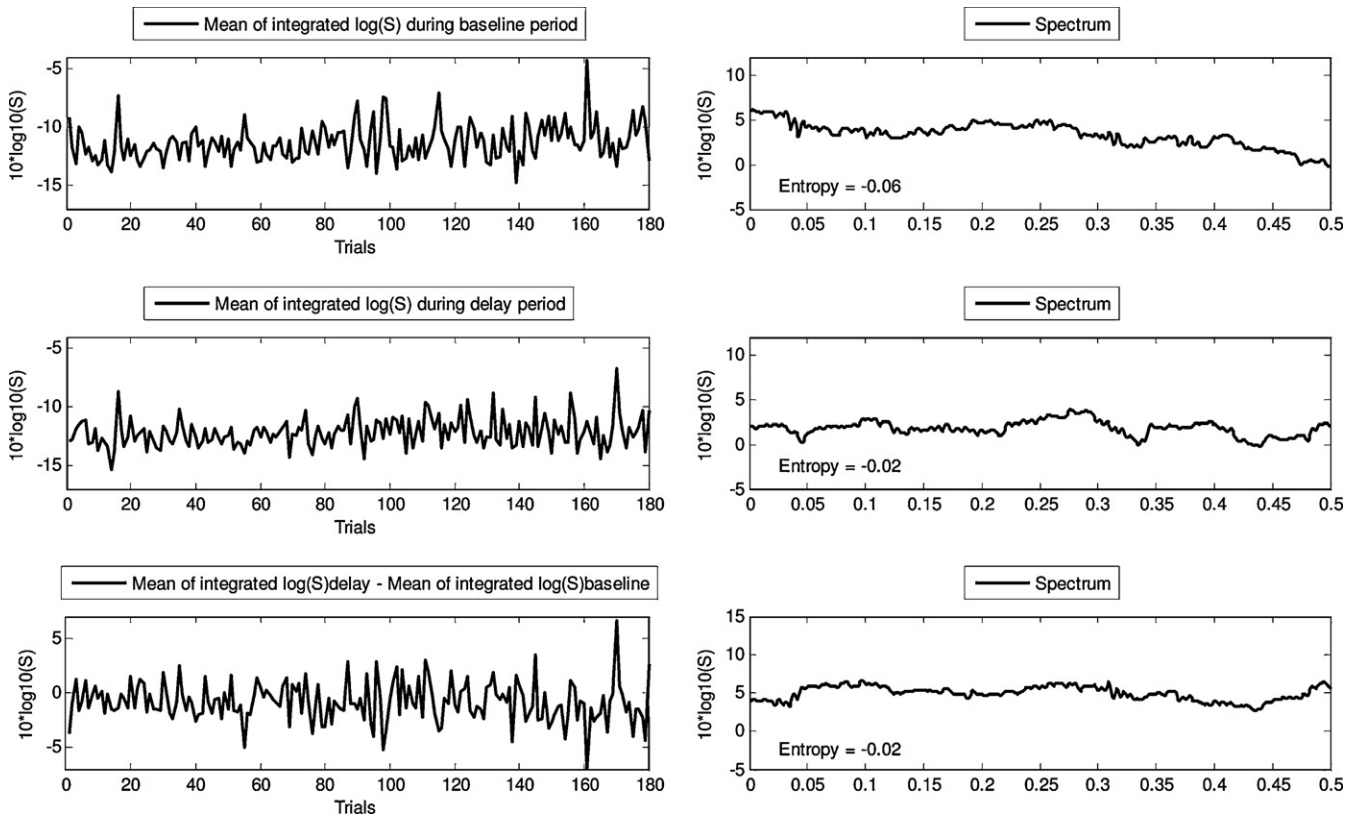


**Fig. 9.** Absence of correlated power variations from trial-to-trial at higher frequencies. This figure represents an atypical result of our analysis for the 60–90 Hz frequency band. These results were seen on 5/27 recordings. This plot shows power variations in the 60–90 Hz range on a different day of recording from the one used in Figs. 7 and 8. Left column shows the average log power during the baseline (top) and delay (middle) periods of 180 trials. The difference between average log power on each trial’s delay vs. baseline periods is shown in the bottom left panel. Right column shows the spectrum of trial-to-trial fluctuations in log power observed during the baseline (top) and delay (middle) periods of the task. Note the absence of long-term trends in log power during baseline and delay periods over the course of the experiment.

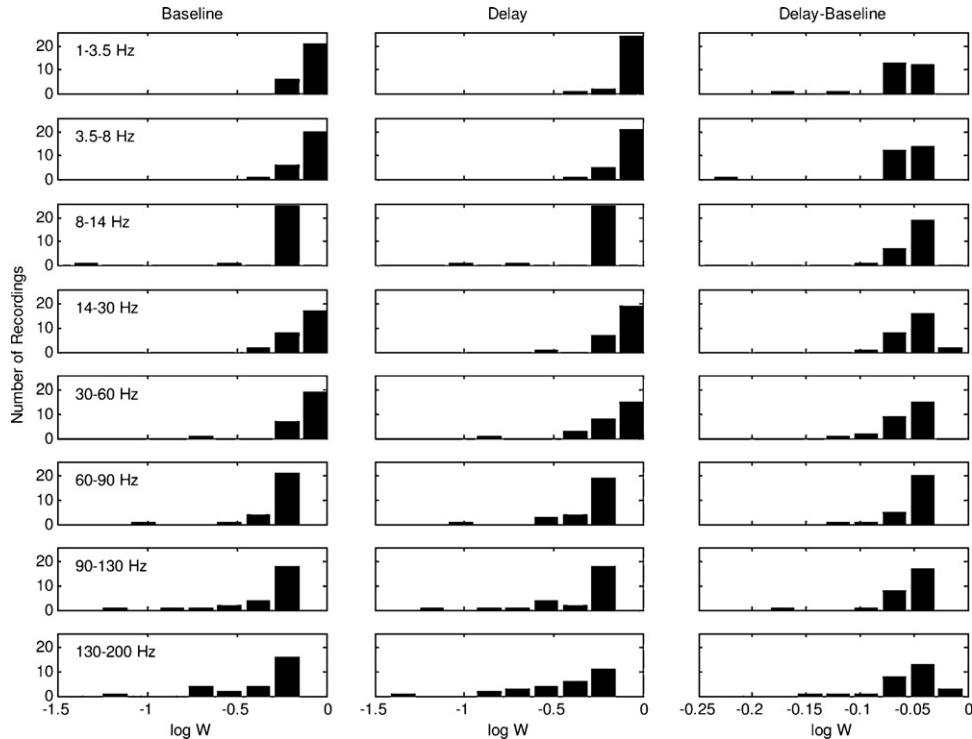


**Fig. 10.** Summary of correlated power variations from trial-to-trial. This figure shows the distribution of Wiener entropy values for the entire dataset of 27 recordings. The rows of the figure show the Wiener entropy values for each of the 8 different frequency bands of the log spectra of trial-to-trial fluctuations. Wiener entropy values for the baseline, delay and the difference between delay vs. baseline are shown in the left, middle, and right columns, respectively. Note that correlated trial-to-trial variability is more common at frequencies above 30 Hz. Also, the distribution of Wiener entropies for the difference between delay vs. baseline log power is clustered near zero, indicating that the correlated log power fluctuations occur comparably during both baseline and delay periods of the behavioral task. The range of Wiener entropies plotted in the right column are from 0 to –0.25 whereas the range for the left and middle columns is from –1.5 to 0.

two states, each describable by a Gaussian process with two different spectra. For example, if in one state the spectrum is white, and in another state the spectrum is piecewise constant (with different constants in different frequency intervals), then the spectral power correlations computed over times longer than the state switching times would show blocks of significant correlations corresponding to the different frequency intervals in question.

Gaussian processes are fully characterized by their spectra (and in the case of multivariate Gaussian processes, the cross-spectral matrix). The spectra form sufficient statistics for Gaussian distributions (assuming zero mean). However, for non-Gaussian processes, higher order moments that are not derivable from the spectra may be defined. These provide additional information about the process that is not captured in the spectra or cross-spectra, and hence are of potential physiologic value. Tests for Gaussianity are important, since they establish conditions under which it is sufficient to characterize the process in terms of the second moments only (spectra or cross-spectra).

#### 4. Conclusions

This study shows that the signal power in LFP recordings obtained from the frontal cortex of an alert behaving rhesus macaque monkey fluctuates on a trial-to-trial basis in a temporally correlated fashion. These findings refute the assumption that trial-to-trial variability in neuronal activity is consistent with a Gaussian stochastic process. This study also shows how correlated trial-to-trial fluctuations can lead to a violation of the assumptions of common statistical methods for comparing the signals recorded under different interleaved behavioral conditions.

#### Acknowledgements

We thank Jonathan D. Victor, Judith A. Menzer, and two anonymous reviewers for helpful comments on an earlier draft of the manuscript. We thank Eugene Weigel for expert animal han-

dling. This work was supported by NIH grant EY007138, NIH grant MH71744, NIH grant MH062528, and CSH Internal Support.

#### References

- Arieli A, Sterkin A, Grinvald A, Aertsen A. Dynamics of ongoing activity: explanation of the large variability in evoked cortical responses. *Science* 1996;273:1868–71.
- Biswal B, Yetkin F, Haughton V, Hyde J. Functional connectivity in the motor cortex of resting human brain using echo-planar MRI. *Magn Reson Med* 1995;34:537–41.
- Eisenhart C. The assumptions underlying the analysis of variance. *Biometrics* 1947;3:1–21.
- Elul R. The genesis of the EEG. *Int Rev Neurobiol* 1972;15:227–72.
- Fox MD, Corbetta M, Snyder AZ, Vincent JL, Raichle ME. Spontaneous neuronal activity distinguishes human dorsal and ventral attention systems. *Proc Natl Acad Sci USA* 2006a;103(26):10046–51.
- Fox MD, Snyder AZ, Zacks JM, Raichle ME. Coherent spontaneous activity accounts for trial-to-trial variability in human evoked brain responses. *Nat Neurosci* 2006b;9(1):23–5.
- Goldman-Rakic PS. Circuitry of primate prefrontal cortex and regulation of behavior by representational memory. In: Plum F, Mountcastle VB, editors. *Handbook of physiology*, vol. 5. Washington, DC: American Physiological Society; 1987. p. 373–517.
- Hasegawa RP, Blitz AM, Geller NL, Goldberg ME. Neurons in monkey prefrontal cortex that track past or predict future performance. *Science* 2000;290:1786–9.
- Hudson AE. Attentional modulation in primate visual area V4. Doctoral dissertation, Cornell University; 2006. Dissertation Abstracts International (UMI No. 3251744).
- Leopold DA, Murayama Y, Logothetis NK. Very slow activity fluctuations in monkey visual cortex: implications for functional brain imaging. *Cerebral Cortex* 2003;13:423–33.
- Llinás RR, Ribary U, Jeanmonod D, Kronberg E, Mitra PP. Thalamocortical dysrhythmia: a neurological and neuropsychiatric syndrome characterized by magnetoencephalography. *Proc Natl Acad Sci USA* 1999;96:15222–7.
- Mitra PP, Pesaran B. Analysis of dynamic brain imaging data. *Biophys J* 1999;76:691–708.
- Nuñez PL. Neocortical dynamics and human EEG rhythms. New York: Oxford University Press; 1995.
- Papadimitris E, Politis DN. Local block bootstrap. *C R Acad Sci Paris Ser I* 2002;335:959–62.
- Percival DB, Walden AT. Spectral analysis for physical applications: multitaper and conventional univariate techniques. Cambridge, UK: University Press; 1993.
- Thompson DJ. Spectrum estimation and harmonic analysis. *Proc IEEE* 1982;70(9):1055–96.
- Vincent JL, Snyder AZ, Fox MD, Shannon BJ, Andrews JR, Raichle ME, et al. Coherent spontaneous activity identifies a hippocampal-parietal memory network. *J Neurophys* 2006;96(6):3517–31.
- Vincent JL, Patel GH, Fox MD, Snyder AZ, Baker JT, Van Essen DC, et al. Intrinsic functional architecture in the anesthetized monkey brain. *Nature* 2007;447:83–6.